THE PENNSYLVANIA STATE UNIVERSITY
SCHREYER HONORS COLLEGE

DEPARTMENT OF METEOROLOGY AND ATMOSPHERIC SCIENCE

Impacts of Growth Kinetics on Heterogeneous and Homogeneous Freezing in Simulated Cirrus

GABRIELLE OLSON
SPRING 2023

A thesis
submitted in partial fulfillment
of the requirements
for a baccalaureate degrees
in Meteorology and Atmospheric Science and Science
with honors in Meteorology and Atmospheric Science

Reviewed and approved* by the following:

Jerry Y. Harrington
Professor of Meteorology
Thesis Supervisor

William H. Brune
Professor of Meteorology
Honors Adviser

* Signatures on file in the Schreyer Honors College.

ABSTRACT

Most numerical models of cirrus clouds utilize a constant deposition coefficient, a quantity related to the efficiency of attachment of water vapor to an ice crystal as it grows. Another assumption made by most cirrus cloud models is that ice forms and grows in the shape of a solid sphere. Unfortunately, these assumptions are not consistent with laboratory measurements. Using a theory of ice growth consistent with lab measurements and a Lagrangian microphysical parcel model, I studied more realistic ice cloud modeling though the incorporation of a varying deposition coefficient and more realistic ice crystal shapes. Throughout my research, I found that varying the deposition coefficients of ice crystals to simulate rosettes, a more realistic ice crystal shape, produced growth different to that of the previously assumed spherical crystals. In fact, rosettes were found to grow closer to column crystals than plate crystals or spherical crystals. The rosette growth is faster, depleting the supersaturation at a greater rate, than spherical growth. Consequently, homogeneous freezing is shut off sooner and at a lower altitude. This result may explain the lower ice concentrations found observationally in cirrus clouds compared to those found in models.

TABLE OF CONTENTS

LIST OF FIGURES

ACKNOWLEDGEMENTS

I would like to thank Dr. Jerry Harrington and Dr. William Brune for their guidance advising and supervising my research. Both greatly fostered my intellectual curiosity and the development of scientific research skills. I am also thankful to the Pennsylvania State University and its Meteorology and Atmospheric Science Department for providing me with the fundamental knowledge of general atmospheric motion and cloud physics. Additionally, I would like to express my gratitude to the National Science Foundation for its financial support as this research was supported, in part, by Grant (*AGS-212834)*. However, I would like to acknowledge that the findings and conclusions of this research do not necessarily reflect the views of the National Science Foundation. Finally, I am grateful for my dog Toby, for I would not be the person I am today without his unconditional love and support.

Chapter 1

Introduction and Background

Ice crystal growth influences the development and evolution of atmospheric cold clouds, which form in the atmosphere where temperatures exist below the melting point of water (0 ^{o}C). An example of a cold cloud would be a cirrus cloud, a cloud consisting solely of ice crystals. Since water vapor is a prevalent component of the atmosphere, one can assume that air parcels within regions primed for atmospheric cold cloud development consist of water vapor. Under such conditions, the water vapor in these parcels can nucleate into ice crystals in various ways. The resulting ice crystals grow through a process called vapor deposition: water vapor deposits onto the ice crystals causing an increase in ice crystal mass and the development of various crystal shapes. Therefore, an important mechanism within atmospheric cold cloud evolution is the formation and growth of ice crystals. The nucleation of ice crystals controls the concentration of ice crystals; however, since nucleation depends on the ambient vapor amount, the vapor growth of crystals can feedback to the nucleation rate.

The resulting ice concentration within cold clouds influences both weather and climate. As ice mass increases through ice crystal vapor growth, the amount of supersaturated water vapor within the air parcel decreases. Therefore, lower ice concentrations within an air parcel equates to a smaller sink of water vapor to deplete the available supersaturated water vapor within the parcel. As a result, lower ice concentrations lead to larger ice crystal sizes (on average) within cold clouds. In fact, vapor growth can produce precipitation-size ice particles, meaning ice concentration can indirectly influence precipitation (Pruppacher and Klett, 1997)

through increases in ice particle fall speeds (Chen and Lamb, 1994). Ice crystal concentrations in cirrus also have impacts on a global scale. Due to the difference between the optical properties of liquid droplets and ice crystals, cold clouds generally have lower albedo than liquid-phase clouds. However, ice clouds can have a range of concentrations and, therefore, radiative effects for ice clouds are dependent on the dominant nucleation mechanism. Homogeneous freezing of solution droplets tends to produce high concentrations of small ice crystals, leading to optically thick clouds that scatter radiation effectively. In contrast, heterogeneous nucleation on ice nuclei produces much lower concentrations, larger crystals, and more tenuous cloud layers with smaller optical thickness. Consequently, larger ice concentrations in cold clouds influence global climate through Earth's radiative budget by reducing absorbed solar radiation. Despite the importance of ice crystal growth and ice concentration to the evolution of cirrus, the details of ice growth are not well understood.

1.1 Limitations of Prior Studies

In an attempt to demystify ice nucleation and other aspects of ice crystal growth, prior studies have been done to examine the impacts of ice nucleation and growth on cirrus. The results of laboratory measurements show that ice crystals nucleate in two different ways: homogeneous freezing and heterogeneous freezing (Demott et al., 1994). While many of these models focus primarily on the impact of homogeneous freezing, a few studies address the competition effect between homogeneous freezing and heterogeneous freezing within an air parcel (Demott et al., 1997; Jensen et al., 2013; Kärcher et al., 2022). Prior studies showed the strong impacts that heterogeneous freezing can have on the homogeneous freezing of solution

drops in cirrus simulations. However, laboratory measurements and other evidence has grown over the years and now indicates that some of these studies had significant limitations.

All parcel models are limited because the vertical motions are fixed, there is no mixing with the surrounding environment, and all ice and liquid particles move with the parcel (i.e. there is no sedimentation). Earlier parcel studies are also limited by the assumptions they make about nucleation and growth. One limitation of most parcel models is an explicit assumption that ice crystals grow in the shape of solid spheres (e.g. Gierens, 2003). Another limitation is that the deposition coefficient, which quantifies the attachment efficiency of water vapor to an ice crystal as it grows, is assumed to be constant. In most parcel and cloud models, the deposition coefficient is assumed to be unity. In this case, ice crystals are assumed to experience perfectly efficient growth. However, the deposition coefficient cannot be unity for faceted crystals, for which the deposition coefficient is less than unity and depends on temperature and supersaturation. Many studies account for a lower deposition coefficient by fixing it to a value of 0.1 or less (Gierens, 2003). While this assumption is more appropriate, measurements and ice crystal growth theory indicate that ice crystals grow with evolving habits, which only occur through varying deposition coefficients (Chen and Lamb, 1994). Unfortunately, very few studies incorporate a varying deposition coefficient (Zhang and Harrington, 2015).

1.2 Incorporation of Laboratory Measurements

In concert with the conclusions derived from ice crystal growth theory, laboratory experiments indicate that realistic ice crystals have varying deposition coefficients and can grow in shapes other than solid spheres. The deposition coefficient is a quantity related to the

efficiency of attachment of water vapor to a facet, basal or prism, of an ice crystal as it grows. As such, the deposition coefficients must vary because the deposition coefficients must be bigger on the actively growing facet. Since growth occurs more efficiently on one facet compared to another, different shapes of ice crystals can form, such as columns or plates. Experimental evidence of varying deposition coefficients comes from laboratory measurements that show that the deposition coefficient is a function of supersaturation (Nelson and Knight, 1998). Therefore, low supersaturations are associated with low deposition coefficients, and the deposition coefficient rises commensurately with supersaturation. During parcel ascent, the ice crystal nucleation and growth in combination with vertical motion causes variations in the supersaturation. Consequently, the deposition coefficients of ice crystals also vary as a parcel is lifted and ice nucleates within the parcel. As such, it is important to incorporate a varying deposition coefficient into numerical models of cirrus clouds.

Another conclusion of lab experiments is that, at high supersaturations, realistic ice crystals have a magnified habit effect: growth rates are enhanced compared to a solid sphere. Ice crystal growth theory indicates that ice crystals can grow in many shapes, including isometric crystals (spheres), planar crystals, columnar crystals, and even other forms of polycrystalline shapes. For high supersaturations, a commonly observed shape within laboratory experiments is a “budding” rosette: an ice core with branches protruding from the core (Figure 1). This shape arises in a high supersaturation environment because multiple nucleation centers usually occur during drop freezing. The initially spherical ice crystal, therefore, develops protruding columnar-like branches with hollow regions called “secondary habits.” The complex shape of these crystals produces relatively high ice crystal growth rates (Pokrifka et al., 2023). As a result, high supersaturations, which are common in cirrus clouds (Krämer et al., 2020), produce ice crystals

that form in the shape of rosettes rather than solid spheres (see Pokrifka et al., 2023; Lawson et al., 2019). Consequently, accurate numerical models of cirrus clouds should incorporate this magnified habit effect and a more realistic ice crystal shape, a rosette.

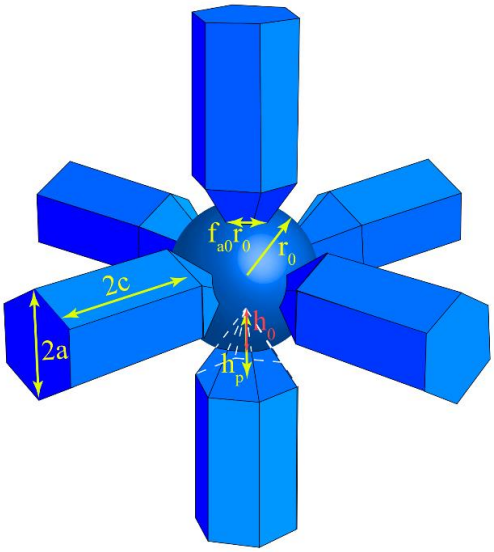

Figure 1. Rosette Ice Crystal Shape (from Pokrifka et al., 2023).

1.3 The Current Work

For the work presented, a numerical parcel model was used to re-examine the competition between heterogeneous freezing and homogeneous freezing with more realistic vapor growth. This work is especially important as the competition effect is very sensitive to vapor growth. In the following sections, I describe the model used for this experimental study and the ice crystal growth theory incorporated into the model. For section 3.1, I use control simulations to describe the influence of the deposition coefficient on spherical ice crystal growth. In sections 3.2-3.4, I explain ice crystal growth of different shapes, including planar crystals, columnar crystals, and rosette crystals. I end in section 4 with a summary of my findings and concluding remarks.

Chapter 2

Methods and Analysis

2.1 Model Description

I conducted simulations using a modified version of the Lagrangian microphysical parcel model described by Zhang and Harrington (2015). In theory, a Lagrangian model follows a parcel of air, with a set of intrinsic characteristics, as the parcel is lifted within a specified vertical range of the atmosphere. Connecting theory and experimental data to cloud processes requires the ability to simulate the growth of individual particles. For that reason, the model separates liquid and ice phase particles into different bins each of which has different particle properties, such as number concentration, particle dimensions, particle density, and fall speed. This homogeneity allows one to numerically solve differential equations that describe parcel evolution and particle growth. Summing the content and size of each bin produces the output of the simulation: the total ice concentration and the average dimensions of the crystals.

This particular form of Lagrangian microphysical model simulates the growth of liquid and ice crystal populations formed by different freezing mechanisms. Consequently, the specific particle properties separating the different bins are liquid mass and ice mass. Throughout the simulation, the growth of both liquid droplets and ice crystals within the parcel are tracked and calculated using the variable ordinary differential equation (VODE; Brown et al., 1989) solver. As particles are nucleated, the model generates n_l and n_i bins of liquid and ice, respectively. For this model, n_l is fixed at a value of 200 since the liquid size distribution is based on a pre-existing soluble cloud condensation nuclei (CCN) spectrum. The number of ice bins, n_i, is determined by the nucleation rate and never creates more than about 500 bins, so it is maximized

at a value of 1000. While some Lagrangian microphysical models separate the liquid and ice crystal populations throughout the entire simulation (Sulia and Harrington, 2011), this model exposes the two subpopulations to one another at each time step. This method accounts for the influence of vapor growth between ice and liquid within a parcel, which is important when analyzing the accuracy of, and competition between, different freezing mechanisms.

Even though this method harbors tremendous value for various applications, it is important to note the limitations of this Lagrangian microphysical model. This model accounts for the interaction between ice and liquid subpopulations, can be adjusted to analyze different freezing mechanisms, and incorporates vertical motion. For simplicity, however, the model does not account for sedimentation or entrainment-mixing processes and the vertical motion is fixed. These processes influence the parcel content post-lifting, specifically with regards to the bins containing larger sized ice and liquid particles as those particles would likely sediment out of the cloud layer.

2.2 Freezing Methods of the Model

Within the atmosphere, freezing arises through a process called ice nucleation, which can occur through various mechanisms. Ice nucleation produces an atmospheric ice particle through the development of an ice embryo of critical size. This embryo can be formed from the pure liquid portion of solution droplets or in the presence of different classes of ice nuclei (Lamb and Verlinde, 2011). As one might expect, this difference influences the mechanism for which ice nucleates. The two major mechanisms of ice nucleation are homogeneous freezing and heterogeneous freezing, which occur in solution drops and on insoluble particles, respectively.

Due to the lower activation energy required for the formation of ice in the presence of an insoluble ice nuclei, ice particles formed through heterogeneous nucleation can form at higher temperatures, causing earlier ice crystal formation that can then deplete the available supersaturation at a higher rate than crystals formed through homogeneous nucleation. Because heterogeneous nucleation forms ice early, these crystals generally grow to be larger in size. While this differentiation may seem a purely academic distinction, understanding this difference does have real world applications.

For example, the type of freezing mechanism that dominates in a region of the atmosphere influences whether layered cirrostratus clouds or broken cirrus uncinus clouds form (Harrington et al., 2009). To elucidate, ice formed heterogeneously, due to the increased ability to form ice provided by ice nuclei, leads to lower concentrations. Hence, heterogeneously frozen ice crystals have the potential to grow to larger sizes (on average) as compared to homogeneously frozen ice crystals, which have higher concentrations of ice crystals and smaller particle sizes (on average). Therefore, clouds dominated by heterogeneous ice nucleation produce larger ice particles (on average). The oscillation of atmospheric waves and the decreased buoyancy of these larger particles increases sedimentation within the cloud layer. These sedimented particles can be advected horizontally due to strong vertical wind shear, forming the wispy shape recognizable as cirrus uncinus clouds. In contrast, clouds dominated by homogeneous ice nucleation produce many smaller ice crystals in layers to produce the stratified shape seen in cirrostratus clouds.

Not only is difference in dominant freezing mechanism a cause of variance in cloud shape, but there is also evidence of competition between both mechanisms within an atmospheric cloud layer. Both mechanisms take place in the atmosphere simultaneously and draw from the

same source: water vapor (Demott et al., 1994). Thus, any model that realistically simulates freezing in the atmosphere should incorporate the interaction between both nucleation mechanisms.

To understand how the interaction of these nucleation and growth processes was simulated, it is important to understand the assumptions made for this parcel model. For these simulations, a set of assumptions was made that align with previous parcel model studies (e.g. Zhang and Harrington, 2015). Specifically, the particles are assumed to consist of aqueous ammonium sulfate initially at equilibrium with the ambient vapor. These CCN are distributed log normally across 200 size bins with a geometric mean radius of 0.015 μm. The number concentration, and the geometric standard deviation are assumed to be 150 cm^{-3} and 1.48, respectively, values typical of upper tropospheric conditions (Lin et al., 2002). For simplification, another assumption that a_w is initially equivalent to the relative humidity was made (Kay and Wood, 2008) and varies according to the properties of the solution droplet.

The major difference between the simulations of homogeneous and heterogeneous freezing mechanisms is the parameterization used to calculate the number of ice crystals produced in a given environment. Specifically, the homogeneous freezing mechanism incorporates the calculation of a nucleation rate with the parameterization of Koop et al. (2000). Koop et al.'s parameterization indicates that the homogeneous nucleation rate is driven primarily by changes in the water activity of the solution droplets. This concept makes physical sense because solution droplets that lack insoluble ice nuclei are highly dependent on reaching a critically dilute concentration to form the ice embryo required for the droplet to freeze. Accordingly, two forms of water activity, which is defined as a ratio of water vapor pressures under similar conditions, are used to determine Koop et al.'s nucleation rate: aerosol water

activity, a_w, and the water activity of a solution in equilibrium with ice, a_w^{ice}. As the solution droplets freeze, the simulation produces ice bins according to the method described in Ervens et al. (2011): a new ice bin is initialized when at least 1% of the solution droplets within that size bin are predicted to freeze. As a result, the largest drops freeze first.

In contrast to the homogeneous freezing mechanism, the heterogeneous freezing mechanism used in these simulations incorporates the parameterization of Demott et al. (2010). Demott et al.'s (2010) parameterization is derived from in-situ measurements made using a Continuous Flow Diffusion Chamber (CFDC). Air from outside an aircraft is passing through the CFDC, which is manipulated to produce a constant ice supersaturation. Within the chamber, aerosol particles are exposed to the supersaturated environment and eventually freeze into ice crystals and are, then, counted. Through numerous observations in cold clouds, Demott et al. (2010) developed a parameterization that relates temperature to the number concentration of ice crystals formed at a specific supersaturation. The number concentration of ice crystals is found to be based on both temperature and total number of aerosol greater than a specific radius ($r > 0.5$ micrometers). A major benefit of using Demott et al.'s parameterization to represent the heterogeneous freezing process is that it is based on observational data, is arguably realistic, and is a standard approach used in numerous studies (Demott et al., 2010).

2.3 Ice Crystal Growth Model

Other than the incorporation of the competition between two different freezing mechanisms, this parcel model can be considered more realistic than previous parcel models due to the incorporation of variable deposition coefficients for two crystal dimensions and effective

density. Many parcel models assume a constant deposition coefficient of 1 or 0.1 (e.g. Gierens, 2003); however, experiments show that the deposition coefficients for faceted ice cannot be constant and must vary as a function of temperature, supersaturation, and crystal size (e.g. Nelson and Baker, 1996; Nelson and Knight, 1998). Laboratory evidence shows that a changing deposition coefficient can describe the growth and development of facets. In fact, the deposition coefficient may depend on how a crystal evolves immediately after freezing (e.g. Pokrifka et al., 2020). To elucidate, crystals that grow in atmospheric clouds develop facets over time. This form of growth indicates that the deposition coefficient is initially below unity ($\alpha < 1$). As the facets develop on the crystal, the crystal's growth rate may transition from one that is very efficient to one that is less efficient, thus, decreasing the deposition coefficient even further (Pokrifka et al., 2020). Furthermore, the supersaturation dependence of the deposition coefficient also indicates that the deposition coefficient varies with respect to time. As an air parcel is lifted vertically, the ice crystals within the parcel are exposed to different levels of supersaturation, thus, changing the deposition coefficient experienced by each crystal. The vertically varying supersaturation also indicates that ice crystals form in various shapes. As supersaturation rises, crystals can develop branching arms and hollowed regions. This occurs once the deposition coefficient reaches unity on a crystal facet. Facets cannot remain flat once the deposition coefficient reaches unity, and hollowing and branching will occur. Hollows and branching arms are often called, "secondary habits," which are modifications to the general form of a hexagonal prism. To model these complex shapes, it is important to incorporate a variable called, effective density (Pokrifka et al., 2023).

Another improvement within this parcel model is the calculation of an effective density. Most parcel models assume that the ice crystals grow as solid spheres (Gierens, 2003). While in-

situ images of these crystals sometimes show particles that appear to be solid spheres, this appearance may be deceiving due to the small size of these particles (radii < 50 micrometers). Moreover, ice crystal growth theory indicates that ice crystals likely form in shapes other than spheres, including plates, columns, rosettes, and other shapes. In fact, recent laboratory research shows clear evidence for crystals with "secondary habits" at small crystal sizes (Bacon et al., 2003), where the measured growth rates of small crystals rise above that of a solid sphere, indicating that the ice crystals develop hollowed regions and branches as the growth rates are enhanced within regions of high supersaturations (Pokrifka et al., 2023). Knowing the density, and subsequent mass, of an ice crystal is important to determine the ice crystal growth rate. One way to estimate the mass of a non-spherical ice crystal is to assume a spherical shaped ice crystal with a reduced density called an "effective density": a circumscribing sphere is placed around the crystal and the density is reduced so that the mass matches that of the actual crystal. For example, the calculation of effective density for one ice crystal shape, rosettes, is based on a simple geometric model of a rosette, an ice core with branches protruding from the core. This model was then used to determine an ice crystal growth rate. The model was then used to show that the densities and growth rates derived from lab data have some correspondence to one particular crystal shape. The resulting match proves indirect evidence of budding rosette growth in the experiments along with a way to calculate the growth rate (Pokrifka et al., 2023).

Chapter 3

Results and Discussion

3.1 Control Simulations Based on Previous Studies

To understand the impact of a realistic, varying deposition coefficient as well as a realistic crystal shape on cirrus cloud development, it is important to analyze control simulations. The control simulations in these experiments were run according to the methods discussed in Chapter 2 and use model inputs consistent with previous research. As described in Chapter 1, many current numerical modeling studies of cirrus assume solid spheres of ice and constant deposition coefficients, with the most typical values used being α=1, 0.1, and 0.01 (e.g. Gierens, 2003). Some prior laboratory studies show that the deposition coefficient can be rather low, α<0.01+ (Magee et al., 2006), whereas other studies find that it has rather high values, $\alpha > 0.1$ (Skrotzki et al., 2013). While constant deposition coefficients are not realistic, they are routinely used in cirrus simulations. As such, the control simulations used for this analysis assume solid spheres of ice and constant deposition coefficients (α=1, 0.1, and 0.01).

In line with previous research, the control simulations indicate that the deposition coefficient strongly influences crystal growth. Since the deposition coefficient equates to the efficiency of water vapor attachment to ice particles, the deposition coefficient affects the primary process responsible for the subsequent ice crystal growth. For high deposition coefficients, the surface is highly efficient in taking up vapor and does not provide resistance to the growth process. As a result, the crystal growth is not limited by the rate of attachment but rather by the only other resistance process: diffusion through the gas phase. Thus, high deposition coefficients correspond to *diffusion limited growth*. In contrast, low deposition

coefficients correspond to a surface that is not efficient in taking up vapor, which provides resistance to the crystal growth process as few molecules are incorporated into the crystal. Therefore, the crystal growth is limited by the rate of surface attachment, which is referred to as *kinetically limited growth*. Growth in which both processes (surface kinetics and gas phase diffusion) influence the growth rate are called *"diffusion-kinetics" limited growth*.

Not only does the magnitude of the deposition coefficient influence whether the growth rate is limited primarily by diffusion or kinetics, but it also influences the overall mass growth rate. For non-spherical ice characterized by two dimensions (a and c), the growth rate can be defined through a series of equations (Zhang and Harrington, 2015):

$$\frac{dm}{dt} = 4\pi C(c,a) D(T,p,c,a,\alpha_c,\alpha_a) S_i \tag{3.1}$$

$$D = \left[\frac{RT_\infty}{M_w D_v' e_i(T_\infty)} + \frac{l_s}{M_w k_T' T_\infty}\left(\frac{l_s}{RT_\infty} - 1\right)\right]^{-1} \tag{3.2}$$

$$D_v' = \frac{2}{3}\chi \frac{D_v}{\left(\frac{4D_v\ C}{\alpha_c \overline{v_v} ac} + \frac{C}{C_\Delta}\right)} + \frac{1}{3}\chi \frac{D_v}{\left(\frac{4D_v\ C}{\alpha_a \overline{v_v} a^2} + \frac{C}{C_\Delta}\right)} \tag{3.3},$$

where $\frac{dm}{dt}$ is the mass growth rate, C is the particle capacitance as a function of its size and shape, C_Δ is the particle capacitance with vapor jump (one mean free path above the surface), D is the effective diffusivity, M_w is the molar mass of water, l_s is the enthalpy of sublimation, R is the universal gas constant, e_i is the equilibrium vapor pressure over ice, S_i is the ambient supersaturation relative to ice, T_∞ is the ambient temperature, p is the pressure, c is the prism axis semi-length, a is the basal axis semi length, α_c is the prism facet deposition coefficient, α_a is the basal facet deposition coefficient, D_v is the vapor diffusivity, D_v' is the modified vapor

diffusivity, k_T' is the modified thermal diffusivity, and $\overline{v_v}$ is the mean vapor molecule speed (see Harrington et al. (2019) for a full description of the equations). Spherical ice crystals are described by Equations 3.1-3.3 when $a = c$. As defined by Equation 3.3, a smaller deposition coefficient on either face of the ice crystal corresponds to a lower effective diffusivity, D_v'. The lower the effective diffusivity, the lower the rate of vapor flow to the crystal. Therefore, the smaller the deposition coefficient, the lower the ice crystal growth rate (see Fig. 6 of Zhang and Harrington, 2015).

The control simulations produce results similar to prior studies (see Gierens, 2003). As the parcel is lifted, ice crystals nucleated heterogeneously grow simultaneously. The growth of the ice particles is evident through the increasing ice water content (Figure 2). At low heights (below 400m), the lowest value of the deposition coefficient (α=0.01) is associated with the lowest growth rate, as indicated by the gradual increase in water content with respect to height (Figure 2). In contrast, the higher values of the deposition coefficient (α=1 and 0.1) initially correspond to greater growth rates, as indicated by the larger increase in water content with respect to height (Figure 2). However, once the parcels reach the homogeneous freezing cloud base, the height at which homogeneous freezing occurs and, thus, ice concentration rises rapidly, (around 520 m in this case) the growth of the crystals with the lowest deposition coefficient (α=0.01) increases rapidly (Figure 2). This result can be explained by the influence of ice crystal growth and vertical motion on the supersaturation.

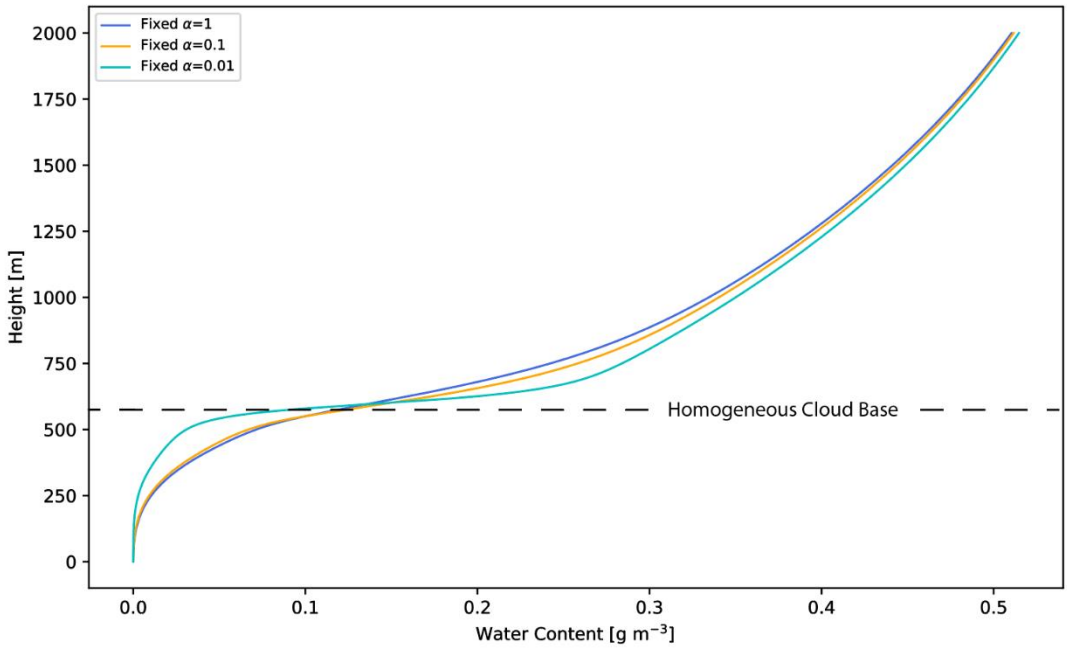

Figure 2. The Effect of Deposition Coefficient on the Growth of Ice Crystals with an Initial Temperature of -30 °C, a Relative Humidity of 78.34%, an Initial Pressure of 400 hPa, an Initial CCN Concentration of 200 CCN per cubic centimeter, and an Ice Nuclei.

Supersaturation depends on the ice crystal growth rate as well as the number of ice crystals nucleated. For example, the time dependency of the supersaturation (S) can be defined as (see Lamb and Verlinde, 2011):

$$\frac{dS}{dt} = Aw - N\frac{dm}{dt} \quad (3.4),$$

where $\frac{dS}{dt}$ is the rate of change of supersaturation with respect to time, A is a function of temperature and pressure, w is the upward wind velocity, N is the number of ice crystals, and $\frac{dm}{dt}$ is the ice crystal growth rate. It is important to note that this equation is an approximation. The equation used in the model integrates the mass growth rate over the size distribution, but for explanatory purposes, the above equation is sufficient. The supersaturation evolution can be described as competition between the source term, Aw, and the sink term, $N\frac{dm}{dt}$. For these simulations, the upward wind velocity is constant (25 cm/s), which means the source term of the

supersaturation rate is approximately constant. The variable in these simulations is the sink term, which consists of the number of nucleated ice crystals and the ice crystal growth rate (Equation 3.4). Figure 3 shows the evolution of the liquid saturation ratio (S) with time, and the liquid supersaturation is directly related to the saturation ratio by $s_u = S-1$. As seen in Figure 3, for a fixed deposition coefficient (α=0.1), the supersaturation at low heights rises almost linearly because the nucleation process has produced very few ice crystals: the source term dominates. At higher altitudes, a significant number of ice crystals nucleate and grow, depleting the supersaturation: the sink term dominates and supersaturation declines (Figure 3). Moreover, the influence of the sink term is clearly evident in the trend of higher initial ice concentrations (5 per liter and 10 per liter): the supersaturation is depleted at a greater rate; specifically, the ice parcel with an initial ice concentration of 10 ice particles per liter shows a significant reduction in the maximum supersaturation (Figure 3).

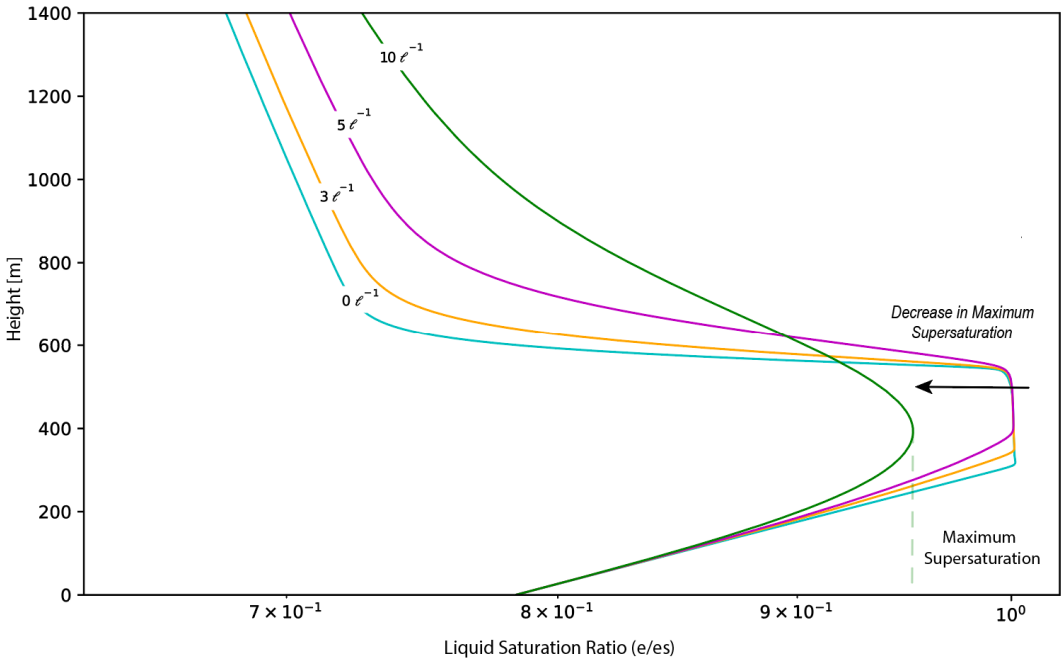

Figure 3. For Fixed α=0.1, The Effect of Initial Ice Concentration on Liquid Supersaturation with Initial Conditions Identical to Those Given in Figure 1. Each colored line corresponds to an initial ice concentration in number of ice crystals per liter.

Changes in the supersaturation rate can explain the rapid increase in ice water content of ice crystals with low deposition coefficients seen in Figure 2. At smaller sizes of ice crystals, the low deposition coefficient suppresses the growth rate for individual ice crystals. As a result, the supersaturation initially rises faster, allowing for the nucleation of a greater number of ice crystals than the simulations with higher deposition coefficients. The sink term depends on both the number of crystals and the growth rate. Consequently, the ice water content rises rapidly in the low deposition coefficient case because the number of nucleated crystals rises rapidly. This result is shown in Figure 2 by the rapid rise in the ice water content of the lowest deposition coefficient, α=0.01. Since higher deposition coefficients increase the growth rate for individual ice crystals, these parcels initially deplete the supersaturation at a higher rate. Fewer ice crystals nucleate in this environment; thus, the ice water content increases less rapidly for higher deposition coefficients (α=1 and 0.1) above cloud base than for the lowest deposition coefficients, α=0.01 (Figure 2). In summary, higher deposition coefficients tend to reduce the number of homogeneously frozen drops within a cirrus cloud.

3.2 Comparing Spherical Crystals to Planar Crystals

As described previously (see Section 3.1 and Equations 3.1-3.3), the growth of single crystalline (hexagonal) ice is described by two dimensions: a and c. The a-dimension of the crystal refers to half the distance across the basal face, and the c-dimension of the crystal refers to half the height of the prism face. These dimensions are often called the “semi-dimensions” of the crystal. The primary habit forms are defined in terms of the ratio of the a and c semi-

dimensions: spherical/isometric crystals arise when φ = 1 (where φ is defined as the ratio a/c), planar crystals arise when φ > 1 and columnar crystals arise when φ < 1 (Figure 4).

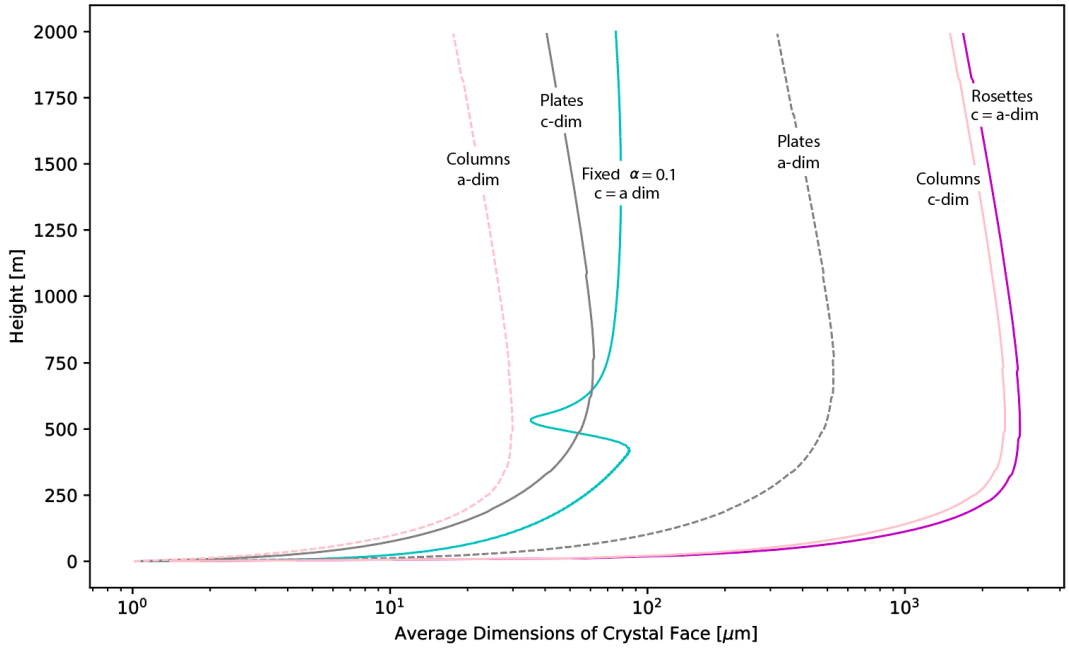

Figure 4. The Effect of Ice Crystal Shape on Average Dimensions of Crystals, Where Each Shape Was Calculated by Using Different Critical Supersaturations for the Basal and Prism Faces. The Initial Conditions are Identical to Those Given in Figure 1.

Different ice crystal shapes result in different growth rates. The relative homogeneity of the surface of a sphere is suitable for three-dimensional growth as the deposition coefficient is fixed and is therefore constant across the surface: vapor is equally likely to attach to all points across the surface. Each face of a planar crystal is associated with a different deposition coefficient (Figure 5). Initially, the deposition coefficient on the basal face of the crystal, α_a, is around 0.01 (Figure 5), making this face highly limited by kinetics. In comparison, the deposition coefficient associated with each of the six prism faces of the crystal, α_a, is almost a magnitude larger at α_a~0.08 (Figure 5), making growth on this face much more efficient. Hence, planar crystals tend to grow “two-dimensionally” because vapor is more likely to attach to any of the prism faces of the crystal rather than either of the basal faces.

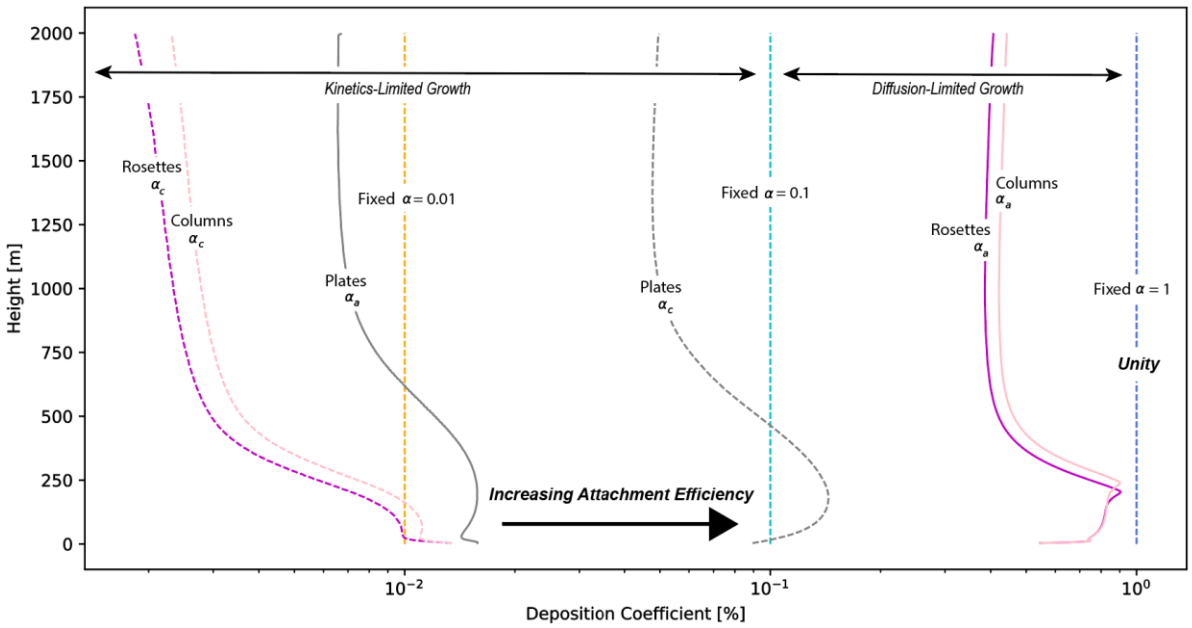

Figure 5. The Effect of Ice Crystal Shape on Deposition Coefficient with Initial Conditions Identical to Those Given in Figure 1. A Smoothing Function, that did not influence the results, was Used to Improve the Visual Interpretation of these Results as the Supersaturation Dependence of the Deposition Coefficient is Highly Sensitive.

While spherical ice crystals can be associated with a fixed deposition coefficient, non-spherical (faceted) ice crystals are only possible with varying deposition coefficients. As seen in Figure 5, the deposition coefficients of spherical crystals, do not vary as the parcel is lifted vertically because these are constant. In contrast, the deposition coefficients associated with all faces of planar crystals and column crystals increases initially, reaches a maximum around 250 m, and decreases (Figure 5). The maximum in the deposition coefficient corresponds to a maximum in supersaturation, which makes sense because the deposition coefficient is supersaturation dependent. Physically, a varying deposition coefficient influences the overall growth rate. At points where the deposition coefficient exceeds 0.1, the planar crystal growth rate exceeds the spherical growth (Figure 6). This rapid increase in the growth rate of planar crystals, increases the sink of supersaturation, and shuts of the process of homogeneous freezing

sooner. As a result, the planar crystal growth eventually (above 550m) trails the growth rate of spherical crystals (Figure 6).

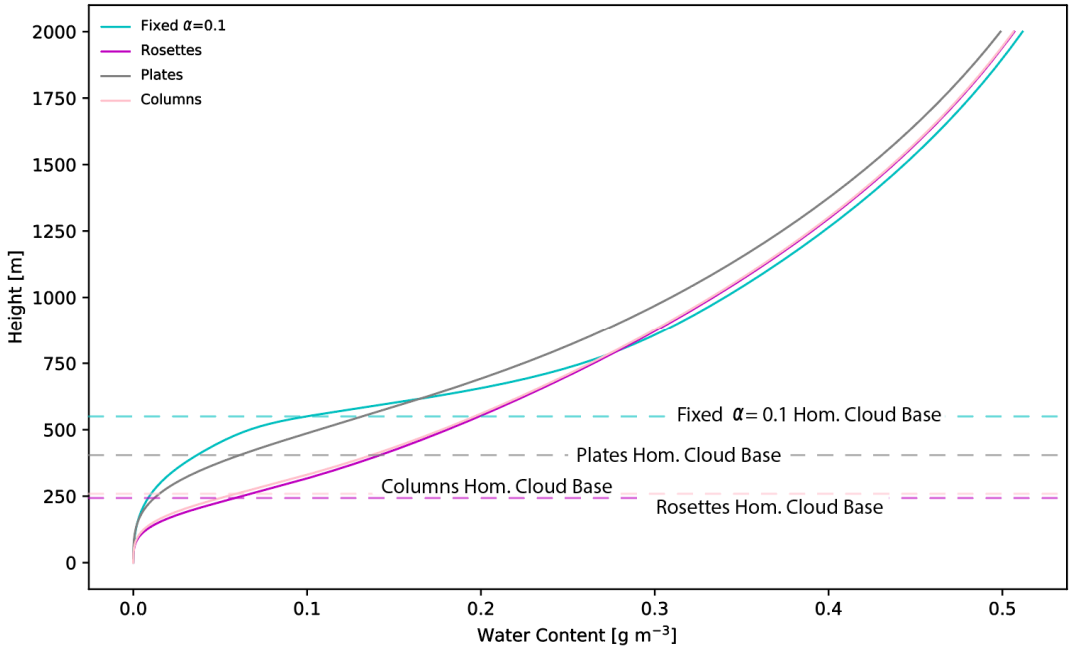

Figure 6. The Effect of Ice Crystal Shape on Ice Water Content with Initial Conditions Identical to Those Given in Figure 1. In the Figure, Hom. Stands for Homogeneous.

3.3 Analysis of Column Crystals

While planar crystals generally grow in a two-dimensional fashion at high supersaturations, column crystals in the same conditions grow one-dimensionally. As mentioned, column crystals are defined by a c-dimension greater than an a-dimension (an aspect ratio > 1). The basal faces of column crystals are small and, therefore, are long and thin. This means that the basal faces extend further into the vapor field and experience higher supersaturations, allowing for vapor to efficiently attach to the basal faces of the crystal. As a consequence, the deposition coefficient of the basal faces of the crystal is greater than that of the prism faces

(Figure 5). As a result, mass attaches to each end of the crystal more efficiently than to all six of the prism faces and growth, therefore, is approximately one-dimensional.

One dimensional growth causes rapid increases in the crystals' length. For columns, the c-dimensional evolution can be derived from the growth rate equation as:

$$c(t) \sim e^{t/\tau_{growth}} \quad (3.4),$$

where c(t) is the c-dimension, t is time, and τ_{growth} is the growth rate timescale. This equation can be derived directly from the mass growth equation if one assumes that the a-dimension does not grow and that all of the mass extends only in the c-dimension. Consequently, the c-dimension within columns grows with high efficiency at an exponential rate; since the deposition coefficient is so high (above 0.1) for the basal face, columnar growth is not limited by surface kinetics and can be described as diffusion limited due to this high attachment efficiency (Figure 5). This can be seen in Figure 4 as columnar crystals grow at a rate greater than both spherical crystals and planar crystals and Figure 6 through the rapidly increasing ice water content. This rapid increase in ice water content significantly increases the supersaturation sink, thus, suppressing homogeneous freezing at a lower altitude than both spherical crystals and planar crystals. While columnar crystals and plate crystals are found in cirrus clouds, polycrystals, such as rosettes, are far more common (Lawson et al., 2019).

3.4 Analysis of Rosette Crystals

In contrast to both column crystals and plate crystals, rosettes are not defined by the relative ratio of the a-dimension and c-dimension of the crystals. In fact, rosettes are modeled in a fashion reminiscent of the assumptions made in the model for spherical crystals: we

approximate the complex structure of a rosette with an enclosing sphere and a reduced density. The geometric shape of the rosette crystals begin as solid spherical ice cores since many of these crystals are formed from frozen solution droplets. Dislocations form during the freezing of the drop, producing a surface with plentiful step sources and high attachment efficiency for the vapor. This freezing process can produce protrusions at the surface, which can lead to the formation of bullets. As a result, protrusions of columnar-like branches grow at these points across the ice core. A method to simplify the modeling for this shape is to assume that the rosette-shaped ice crystals grow with equivalent a- and c-dimensions but to reduce the density of the "sphere" as if to simulate the difference in volume of ice between the branches of the ice crystal and a solid spherical ice crystal. This reduction is accounted for by an effective density.

Figure 4 indicates the dimensional growth of rosette ice crystals is similar to that of the c-dimensional growth of columnar crystals. This rapid dimensional growth influences the evolution of ice water content for both columnar crystals and rosette crystals. Growth in the ice water content of the rosette crystals also follows growth of the ice water content of columnar crystals (Figure 6). This result makes physical sense because the geometric shape of a rosette is simply a series of columnar crystals protruding from a solid ice core. As a result, the growth of rosette ice crystals is akin to the c-dimensional growth of columnar crystals. In fact, the protruding crystals considerably extend into the vapor field, allowing for a greater rate of attachment than columnar crystals (Figure 4 & Figure 6).

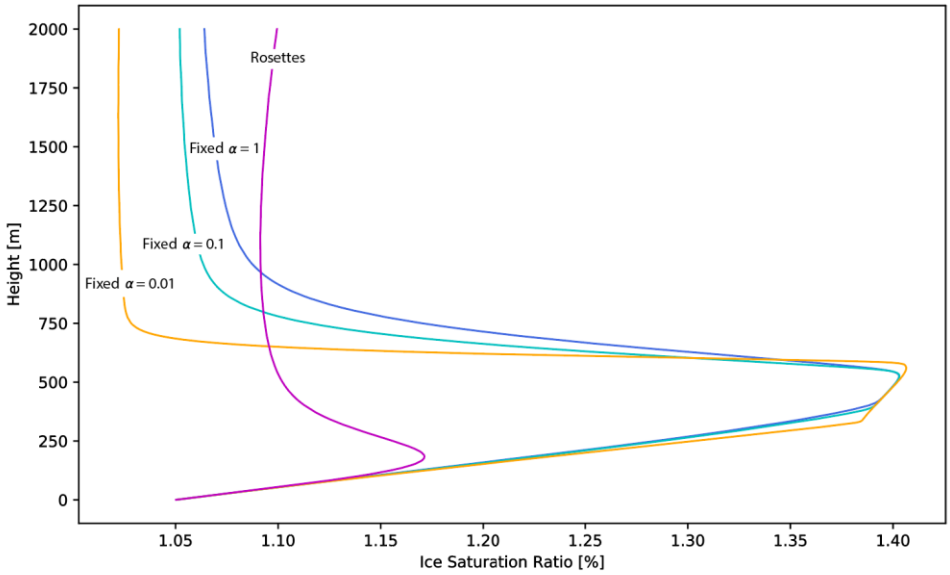

Figure 7. For a Fixed Initial Ice Concentration of 5 Ice Crystals per Liter, The Effect of Ice Crystal Shape on Ice Supersaturation with Initial Conditions Identical to Those Given in Figure 1.

Similar to columnar crystals, the higher deposition coefficients associated with rosette crystals (Figure 5) indicate that growth of rosette crystals is diffusion limited and depletes the supersaturation at a rapid rate. The impact of this rapid growth rate can be seen in Figure 7 as the height at which the sink term of the supersaturation outweighs the source term for rosette ice crystals occurs around 240 m, which is much lower than that of the spherical ice crystals (~450m). This impact influences the competition between heterogeneous and homogeneous nucleation. The rapid growth rate associated with rosette crystals indicates that the parcel need not reach as high of a nucleated ice concentration to suppress homogeneous freezing. For a fixed deposition coefficient, α=0.1, an increase in the number of initially nucleated ice particles led to an increase in the suppression of homogeneous ice nucleation process: as the number of initially nucleated ice particles increased from 0 to 3 to 5 ice nuclei per liter, the number of homogeneously nucleated ice particles decreased (Figure 8). In fact, at an initial ice nuclei concentration of 10 ice nuclei per liter, homogeneous ice nucleation was suppressed at 700 m

(Figure 8). Consequently, the growth of rosette crystals shuts off homogeneous freezing at a lower altitude. In fact, Figure 9 indicates that the homogeneous freezing begins around 390 m for spherical growth, whereas homogeneous nucleation was suppressed even around 700 m for rosette crystal growth.

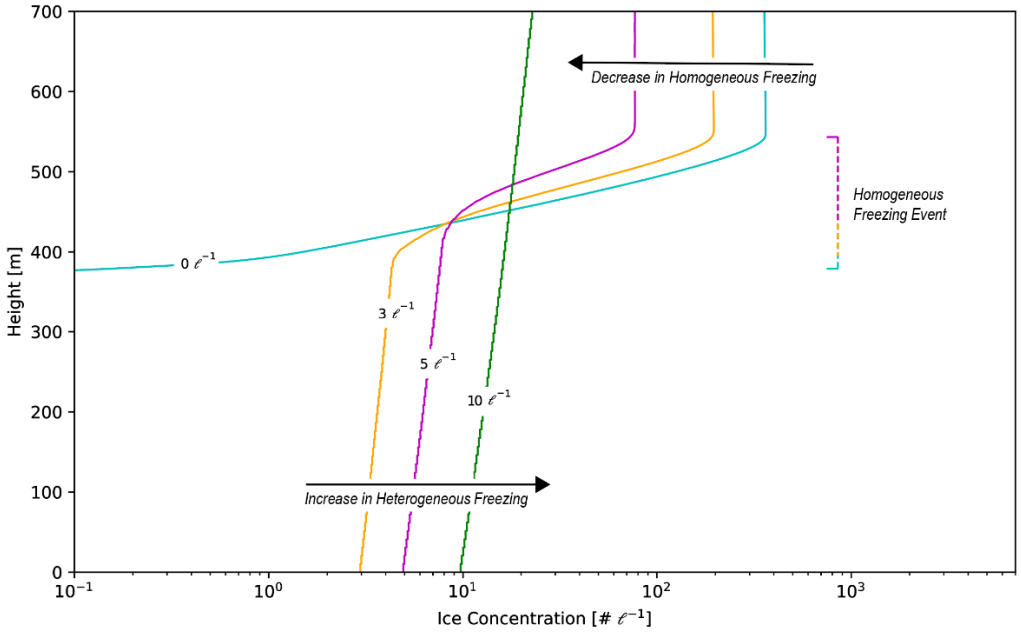

Figure 8. The Effect of Varying the Initial Ice Nuclei Concentration for a Fixed Deposition Coefficient, α=0.1. The Initial Conditions are Identical to Those Given in Figure 1.

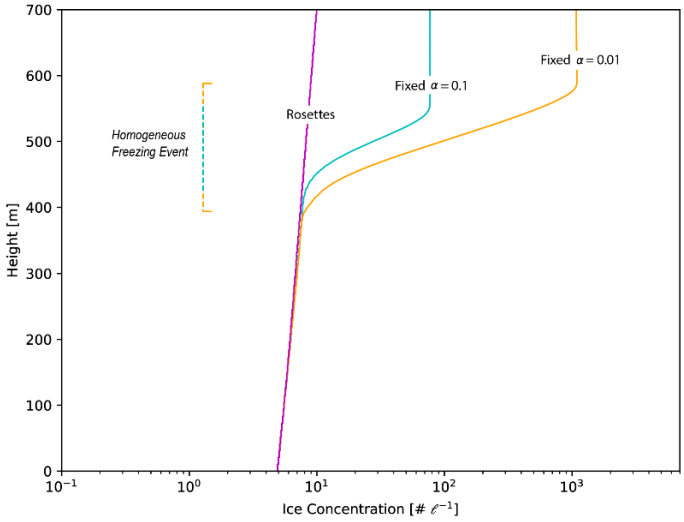

Figure 9. The Effect of Shape on Ice Concentration in Cirrus Clouds with Initial Conditions Identical to Those Given in Figure 1.

The difference in crystal shape has important consequences for the influence of heterogeneous nucleation on the homogeneous freezing process. As was pointed out above, homogeneous freezing will be suppressed once ice nuclei concentrations are high enough. According to Figure 10, the trends described in 3.1-3.4 hold true as crystals growing with higher deposition coefficients suppress the number of ice crystals produced from homogeneous nucleation alone (i.e. no heterogeneous ice nucleation); this occurs, approximately along the left-hand y-axis, since the number of heterogeneous ice nuclei is nearly zero. Note that spherical crystals with the lowest deposition coefficient (α=0.01) have the highest ice concentrations associated with homogeneous nucleation alone and rosette crystals produce the lowest ice concentrations. This makes sense because rosettes have the highest overall growth rates, and this produces the strongest suppression of homogeneous freezing.

The strength of competition between heterogeneous nucleation and homogeneous nucleation mechanisms can be described by the decline of the maximum ice crystal concentration with respect to an increasing ice nucleating (IN) aerosol concentration. In other words, as the IN concentration rises, the sink term for the supersaturation increases, reducing the overall number of nucleated ice crystals. As such, spherical crystals with the lowest deposition coefficient (α=0.01) experience the least suppression of homogeneous freezing by heterogeneous freezing. This result is indicated by the most gradual decline of maximum ice crystal concentration (Figure 10). In contrast, column crystals and rosette crystals experience the greatest suppression of homogeneous freezing by heterogeneous freezing. This result is indicated by the most rapid decline of maximum ice crystal concentration until a minimum value is reached (Figure 10). This minimum in the maximum ice crystal concentration correlates with the height in Figure 7 where the supersaturation sink term overtakes the supersaturation source term.

At this height, an increase in IN concentration linearly increases the maximum ice crystal concentration as all of the crystals are frozen through heterogeneous freezing alone.

Therefore, rosette ice crystals reach the lowest maximum ice crystal concentration of all ice crystal shapes due to a cascade effect. Rosette ice crystals have large, varying deposition coefficients similar to that of columnar crystals, which leads to a larger ice crystal growth rate. Consequently, this growth rate increases the supersaturation sink of the crystal growth. This suppression in supersaturation increases the impact of the competition between heterogeneous nucleation and homogeneous nucleation mechanisms, thus, reducing the maximum ice crystal concentration of rosette crystals attained through ice nucleation mechanisms. These results are significant as noted by the limitations of using constant deposition coefficients (α=0.01-0.1), indicated by the shaded region of Figure 10.

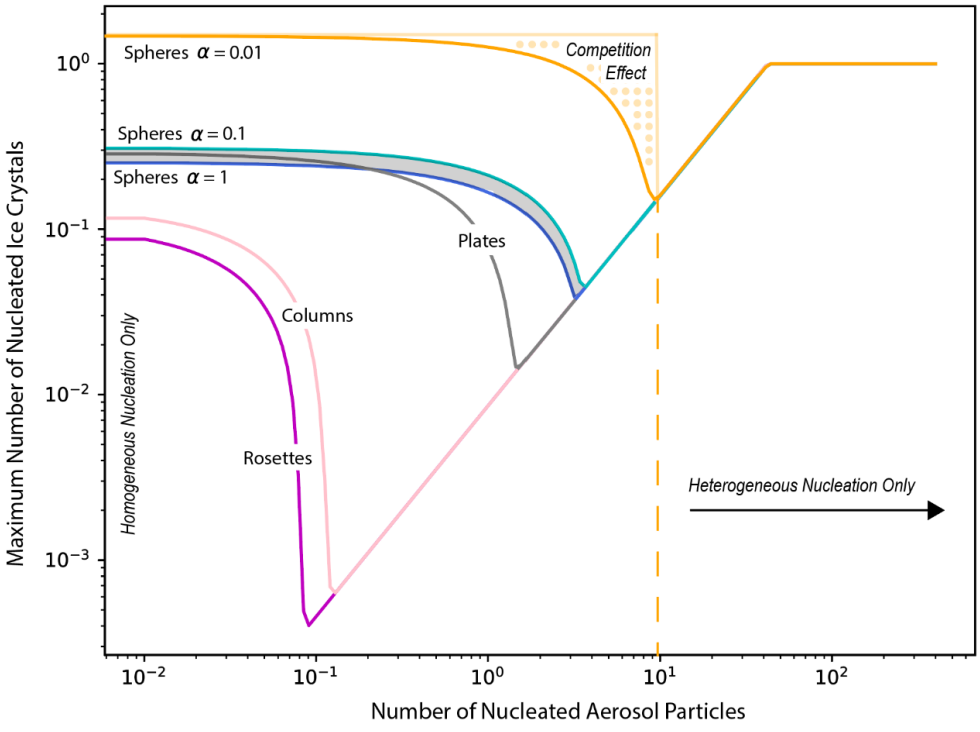

Figure 10. The Effect of Ice Crystal Shape on Nucleation Mechanisms with Initial Conditions Identical to Those Given in Figure 1. The shaded region highlights the limitations of current models.

Chapter 4

Summary and Conclusion

4.1 Summary

As expected, the introduction of a varying deposition coefficient correlating to a realistic ice crystal shape influences the microphysical properties of simulated cirrus. Consequently, this exploratory study assessed the influence of varying deposition coefficients on nucleation rates in cirrus. The main results can be summarized as follows:

1) The higher the deposition coefficient, the lower the number of homogeneously frozen solution drops. Higher deposition coefficients produce larger growth rates, and in combination with heterogeneous freezing, this suppresses homogeneous freezing.
2) Simulations of different ice crystal shapes can be described by deposition coefficients that vary with respect to the height of the parcel as it is lifted, as shown in previous studies (Zhang and Harrington, 2015).
3) Planar crystals exhibit similar competition effects between homogeneous and heterogeneous freezing mechanisms to those of spherical crystals at low concentrations of ice nuclei; however, planar crystals deplete the supersaturation rate at a much faster rate than spherical crystals, reducing the number of homogeneously frozen drops.
4) Columnar crystals grow much faster than planar crystals and spherical crystals due to an exponential growth rate which further reduces the number of homogeneously frozen drops.

5) While the growth of each rosette arm is similar to the high growth rate of columnar crystals, rosette crystals deplete the supersaturation at an even higher rate than all other crystal shapes. The resulting depletion of the supersaturation reduces the number of homogeneously frozen drops as homogeneous freezing is shut off sooner and at a lower altitude than other ice crystal shapes.

4.2 Conclusion

The results in this study indicate the importance of the incorporation of a varying deposition coefficient that is calculated consistently with the rosette ice crystal shape into numerical modeling of cirrus clouds. This adjustment to the numerical model is rooted in the laboratory measurements of Pokrifka et al. (2023) and their theoretical model of a budding rosette crystal. The greater deposition coefficients predicted by the rosette is consistent with the exponential ice crystal growth rate for columnar crystals, which rapidly depletes the supersaturation. This supersaturation depletion suppresses homogeneous freezing significantly, thus reducing the number of homogeneously frozen solution drops.

This result may explain the lower ice concentrations found observationally in cirrus clouds compared to those simulated by cirrus models. Observational studies have indicated low ice concentrations in cirrus clouds (Krämer et al., 2020). These concentrations are, in fact, much lower than the minimum ice concentrations produced by model simulations (Krämer et al., 2020). The realistic shape and varying deposition coefficient associated with rosette ice crystals, when used in parcel model simulations of cirrus, produce reduced values of ice concentration similar to some of these observations. Since these results potentially explain an inconsistency

between models and observations, one can deduce that the incorporation of a varying deposition coefficient corresponding to that of rosette ice crystals into climate model simulations may improve the accuracy of such models.

BIBLIOGRAPHY

Bacon, N. J., M. B. Baker, and B. D. Swanson, 2003: Initial stages in the morphological evolution of vapour-grown ice crystals: A laboratory investigation. *Q.J.R.Meteorol.Soc.*, **129**, 1903-1927, https://doi.org/10.1256/qj.02.04.

Brown, P., G. Byrne, and A. Hindmarsh, 1989: VODE: A variable coefficient ODE solver. *SIAM. J. Sci. Stat. Comput*., **10**, 1038–1051, https://doi.org/10.1137/0910062.

Chen, J., D. Lamb, 1994: The Theoretical Basis for the Parameterization of Ice Crystal Habits: Growth by Vapor Deposition. *J. Atmos. Sci.*, **51**, 1206-1222, doi:10.1175/1520-0469(1994)051.

DeMott, P. J., A. J. Prenni, X. Liu, S. M. Kreidenweis, M. D. Petters, C. H. Twohy, M. S. Richardson, T. Eidhammer, and D. C. Rogers, 2010: Predicting global atmospheric ice nuclei distributions and their impacts on climate. *Proceedings of the National Academy of Sciences*, **107**, 11217-11222, https://doi.org/10.1073/pnas.090818107.

Ervens, B., G. Feingold, K. Sulia, and J. Harrington, 2011: The impact of microphysical parameters, ice nucleation mode, and habit growth on the ice/liquid partitioning in mixed phase Arctic clouds, *Journal of Geophysical Research: Atmospheres*, **116**, https://doi.org/10.1029/2011JD015729.

Gierens, K. M., M. Monier, and J. Gayet, 2003: The deposition coefficient and its role for cirrus clouds. *Journal of Geophysical Research: Atmospheres*, **108**, –4069, https://doi.org/10.1029/2001JD001558.

Harrington, J. Y., A. Moyle, L. E. Hanson, and H. Morrison, 2019: On calculating deposition coefficients and aspect-ratio evolution in approximate models of ice crystal vapor growth. *J. Atmos. Sci.*, **76**, 1609–1625, https://doi.org/10.1175/JAS-D-18-0319.1.

Harrington, J. Y., D. Lamb, and R. Carver, 2009: Parameterization of surface kinetic effects for bulk microphysical models: Influences on simulated cirrus dynamics and structure. *J. Geophys. Res.*, **114**, D06212, https://doi.org/10.1029/2008JD011050.

Jensen, E. J., and Coauthors, 2018: Heterogeneous Ice Nucleation in the Tropical Tropopause Layer. *Journal of Geophysical Research: Atmospheres*, **123**, 12210-12227, https://doi.org/10.1029/2018JD028949.

Kärcher, B., P. J. DeMott P. J., E. J. Jensen, and J. Y. Harrington, 2022: Studies on the Competition Between Homogeneous and Heterogeneous Ice Nucleation in Cirrus Formation. *Journal of Geophysical Research: Atmospheres*, **127**, https://doi.org/10.1029/2021JD035805

Kay, J., and R. Wood, 2008: Timescale analysis of aerosol sensitivity during homogeneous

freezing and implications for upper tropospheric water vapor budgets. *Geophys. Res. Lett.*, **35**, L10809, https://doi.org10.1029/2007GL032628.

Koop, T., B. Luo, A. Tslas, and T. Peter, 2000: Water activity as the determinant for homogeneous ice freezing in aqueous solutions. *Nature*, **406**, 611–614, https://doi.org/10.1038/35020537.

Krämer, M., and Coauthors, 2020: A microphysics guide to cirrus – Part 2: Climatologies of clouds and humidity from observations. *Atmos. Chem. Phys.*, **20**, 12569–12608, https://doi.org/10.5194/acp-20-12569-2020.

Lamb, D., and J. Verlinde, 2011: *The Physics and Chemistry of Clouds*. Cambridge University Press.

Lawson, R. P., and Coauthors, 2019: A review of ice particle shapes in cirrus formed in situ and in anvils. *J. Geophys. Res. Atmos.*, **124**, 10 049–10 090, https://doi.org/10.1029/2018JD030122.

Lin, R. F., D. O'C. Starr, P. DeMott, R. Cotton, K. Sassen, E. Jensen, B. Karcher, and X. Liu, 2002: Cirrus parcel model comparison project. Phase I: The critical components to simulation cirrus initiation explicitly. *J. Atmos. Sci.*, **59**, 2305–2329, https://doi.org/10.1175/1520-0469(2002)059,2305: CPMCPP.2.0.CO;2.

Magee, N., A. Moyle, and D. Lamb, 2006: Experimental determination of the deposition coefficient of small cirrus-like crystals near 2508C. *Geophys. Res. Lett.*, **33**, L17813, https://doi.org/10.1029/2006GL026665.

Nelson, J. T., M. B. Baker, 1996: New theoretical framework for studies of vapor growth and sublimation of small ice crystals in the atmosphere. J. Geophys. Res.: Atmos., **101**, 7033-7047, https://doi.org/10.1029/95JD03162.

Nelson, J., and C. Knight, 1998: Snow Crystal Habit Changes Explained by Layer Nucleation. *J. Atmos. Sci.*, **55**, 1452-1465, https://doi.org/10.1175/15200469(1998)<1452:SCHCEB >2.0.CO;2.

Pokrifka, G. F., A. M. Moyle, J. Y. Harrington, 2023: Effective Density Derived from Laboratory Measurements of the Vapor Growth Rates of Small Ice Crystals at -65 to -40 C. *J. Atmos. Sci.*, https://doi.org/10.1175/JAS-D-22-0077.1

Pokrifka, G. F., A. M. Moyle, L. E. Hanson, and J. Y. Harrington, 2020: Estimating surface attachment kinetic and growth tranisition influences on vapor-grown ice crystals. *J. Atmos. Sci.*, **77**, 2393–2410, https://doi.org/10.1175/JAS-D-19-0303.1.

Pruppacher, H. R., J. D. Klett, 1997: Microphysics of Clouds and Precipitation. 2nd ed. Vol. 18, Kluwer Academic Publishers.

Skrotzki, J., and Coauthors, 2013: The accommodation coefficient of water molecules on Ice. Cirrus cloud studies at the AIDA simulation chamber. *Atmos. Chem. Phys.*, **13**, 4451–4466, https://doi.org/10.5194/acp-13-4451-2013.

Sulia, K., and J. Harrington, 2011: Ice aspect ratio influences on mixed-phase clouds: Impacts on phase partitioning in parcel models. *J. Geophys. Res.*, **116**, D21309, https://doi.org/10.1029/2011JD016298.

Zhang, C., and J. Harrington, 2015: Including surface kinetic effects in simple models of ice vapor diffusion. *J. Atmos. Sci.*, **71**, 372–390, https://doi.org/10.1175/JAS-D-13-0103.1.

ACADEMIC VITA
Gabrielle Olson

EDUCATION

The Pennsylvania State University — University Park Campus
Bachelor of Science in Meteorology and Atmospheric Science — *May 2023 (Anticipated)*
Bachelor of Science in Science
Schreyer Honors College, Thesis Topic: Cirrus Cloud Development
Student Marshal for Department of Meteorology and Atmospheric Science

Mounds View High School — *May 2019*

WORK EXPERIENCE

Intern | Veterinary Cardiology Services — *Dec, May-Aug 2020*

RESEARCH EXPERIENCE

Intern | Penn State University — *Jun-Sep 2021, May-Dec 2022*
- ❖ Research with Dr. William Brune

Volunteer | Penn State University — *June 2022-May 2023*
- ❖ Research with Dr. Jerry Harrington

LEADERSHIP EXPERIENCE

President | Enactus Team at Penn State — *Jan 2022-Present*
Student Executive Committee | Penn State Startup Week — *Dec 2022-Present*
Undergraduate Student Comittee | College of EMS Sustainability Council — *Jun 2021-Present*
Council of Sustainable Leaders | Sustainability Institute at Penn State — *Nov 2020-May 2021*

PUBLICATIONS

Brune, W. H., Jenkins, J. M., Olson, G. A., McFarland, P. J., Miller, D. O., Mao, J., Ren, X. (2022); Extreme Hydroxyl Amounts Generated by Thunderstorm-Induced Corona on Grounded Metal Objects. *PNAS*, *119* (37).

Jenkins, J. M., Olson, G. A., McFarland, P. J., Miller, D. O., Brune, W. H. (2022); Prodigious Amounts of Hydrogen Oxides generated by Corona Discharges on Tree Leaves. *Science*, *127* (16).

VOLUNTEER EXPERIENCE

Forecast Verification | Penn State University — *Nov 2019-May 2021*

CONFERENCES

Global Sustainable Action Conference 2022 | Penn State University — *Nov 2022*
- ❖ Presented at *It Starts with Us* regarding a method to bridge the gap between students as an underutilized resource and the implementation of sustainability into local and global communities

RISE Conference 2019 | University at Albany — *Nov 2019*
- ❖ Invited to attend *Transforming University Engagement in Pre- and Post-Disaster Environments: Lessons from Puerto Rico*

AWARDS

Behrmann Award in Meteorology and Atmospheric Science | Penn State University — *March 2023*
Student Leadership Scholarship | Penn State University — *Dec 2022*